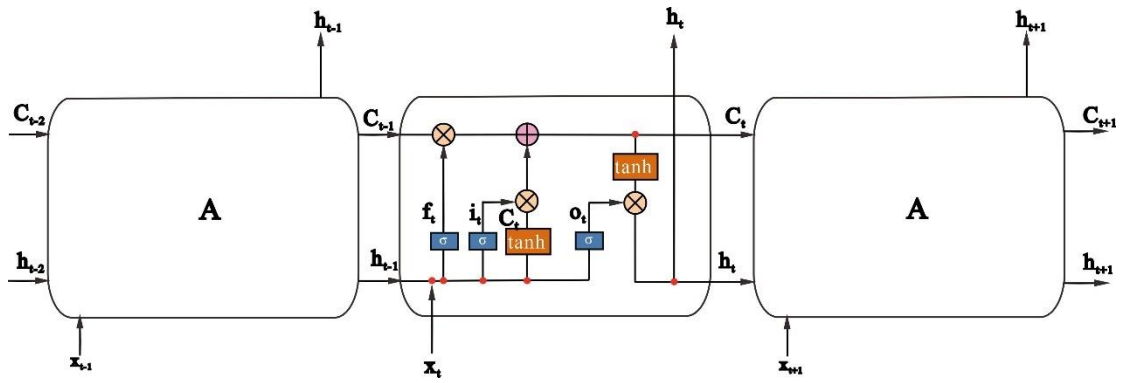
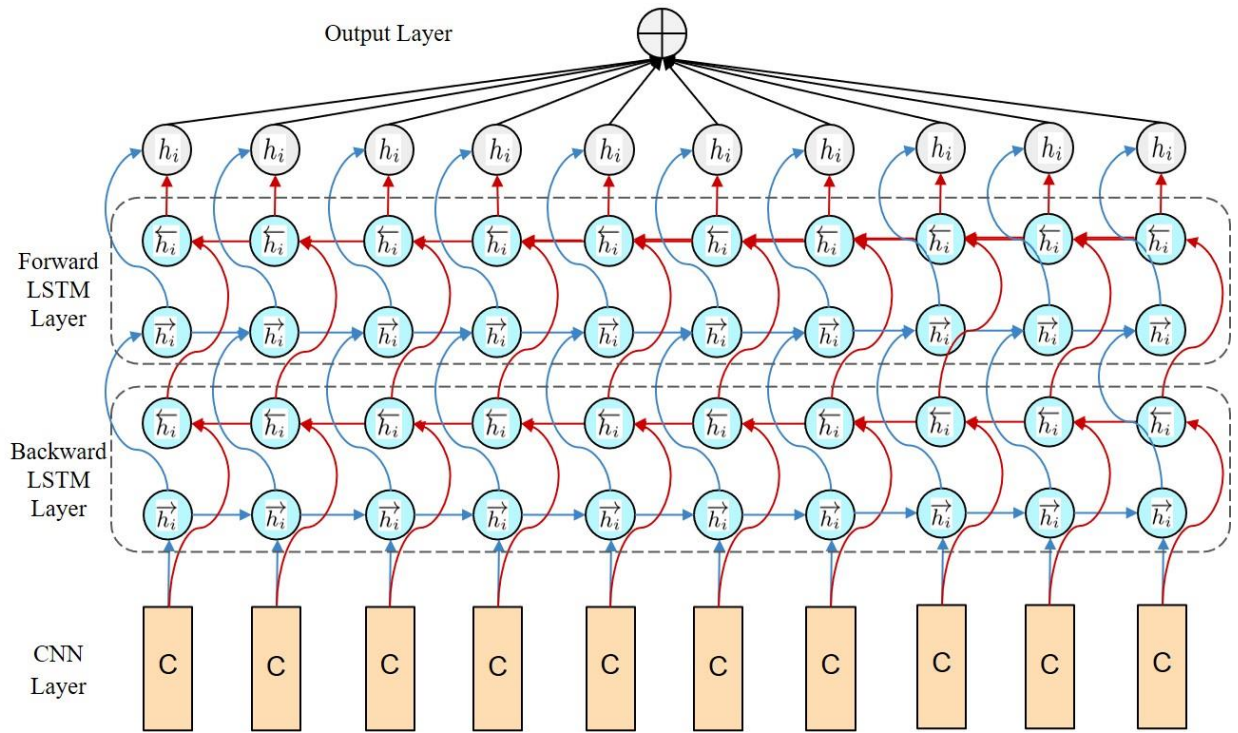


(a) Structure of Convolutional Neural Network.



(b) The memory cell of LSTM.



(c) Schematic diagram of CNN-Bi-LSTM forecasting model.

Fig. 1 The internal structure of the prediction model.

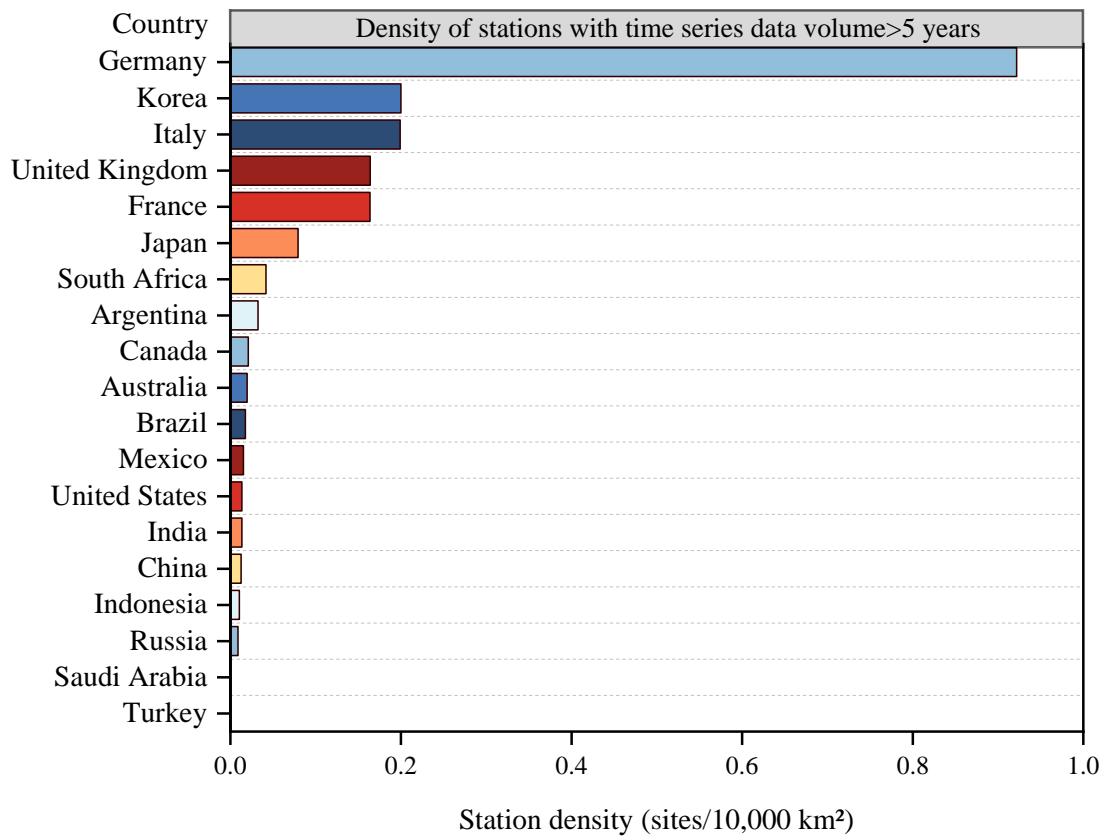


Fig. 2 Isotope data volume statistics for major countries in all regions of the world.

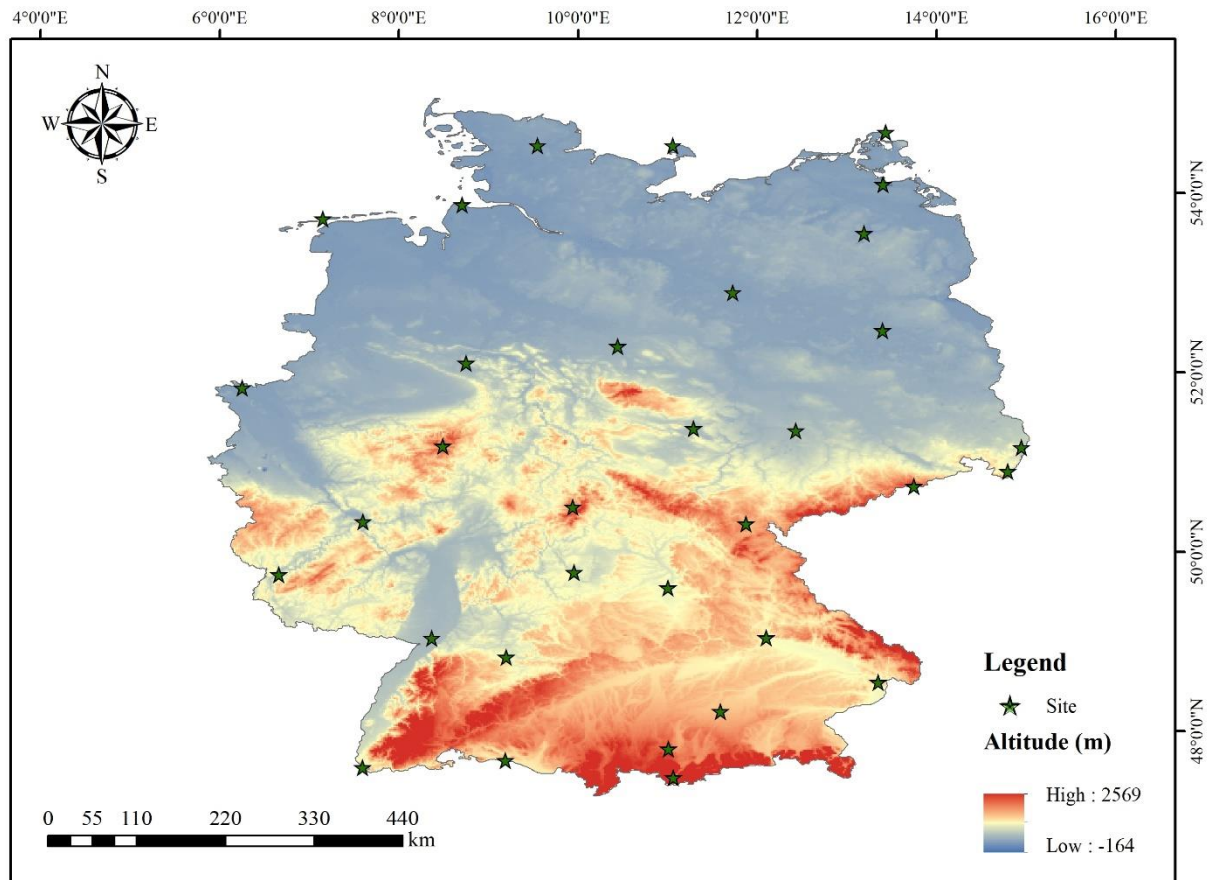
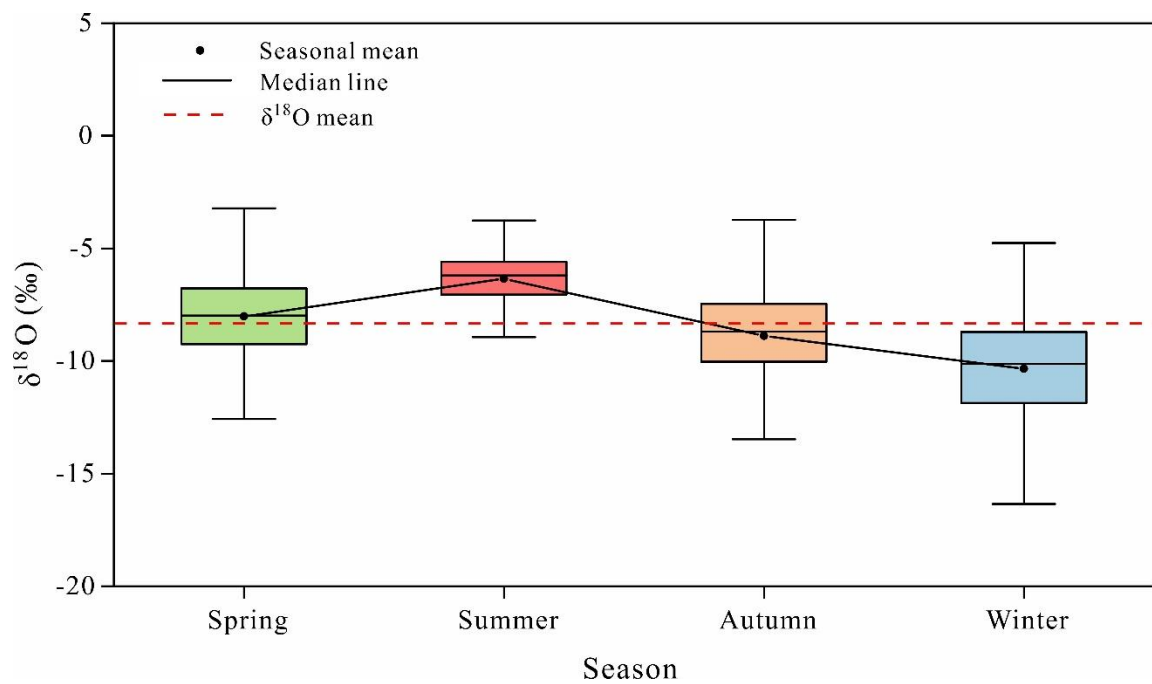


Fig. 3 Location of the study site.



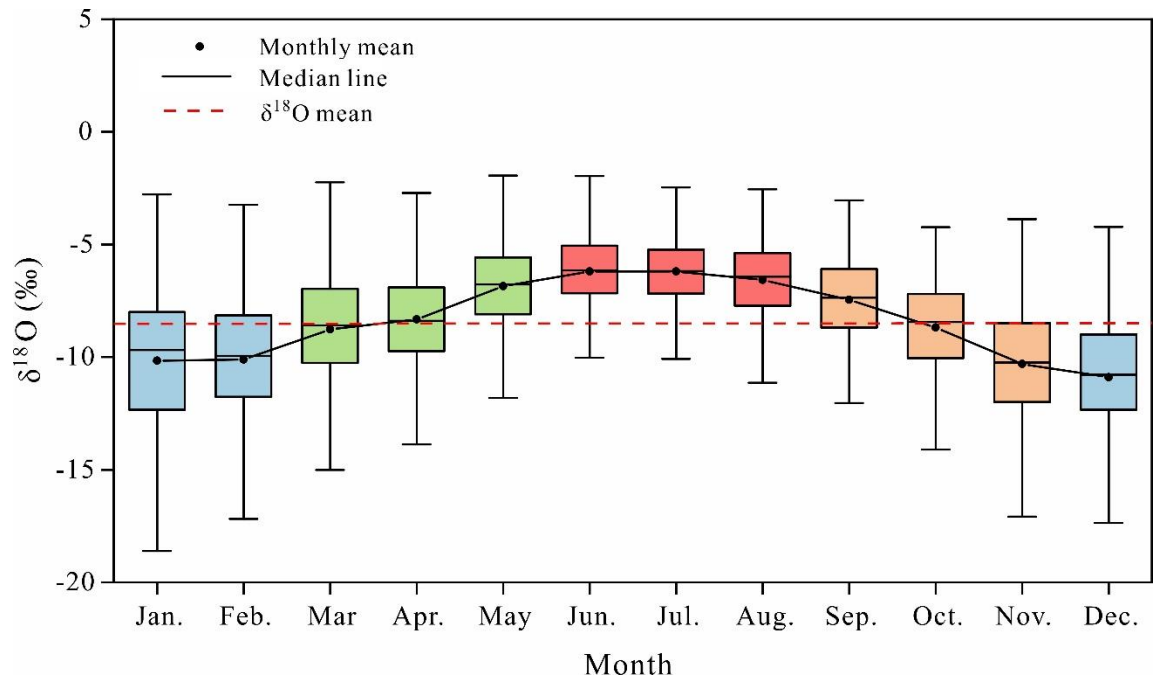


Fig. 4 Temporal distribution characteristics of the precipitation $\delta^{18}\text{O}$.

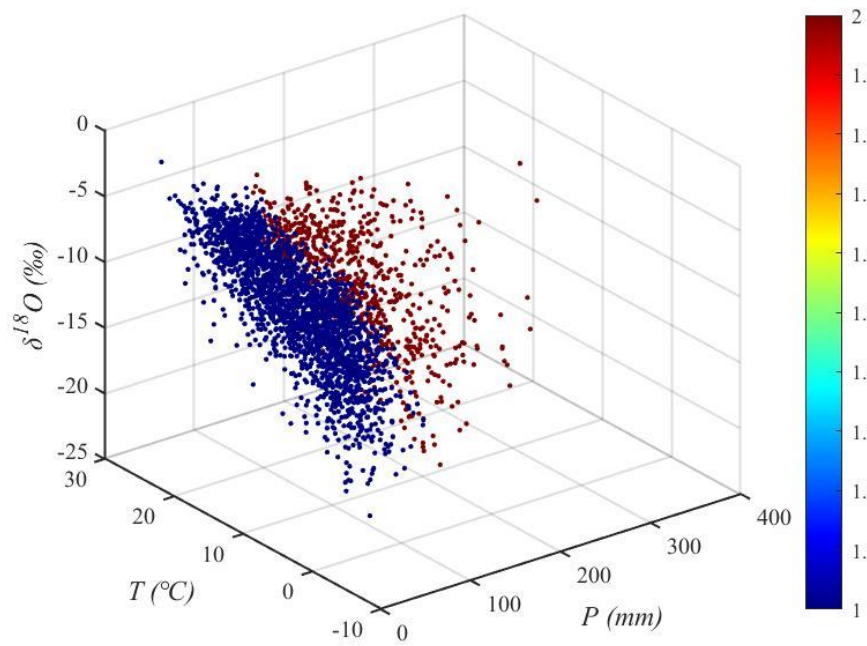


Fig. 5 Spatiotemporal distribution characteristics of the precipitation $\delta^{18}\text{O}$ (Blue represents the first cluster, red represents the second cluster).

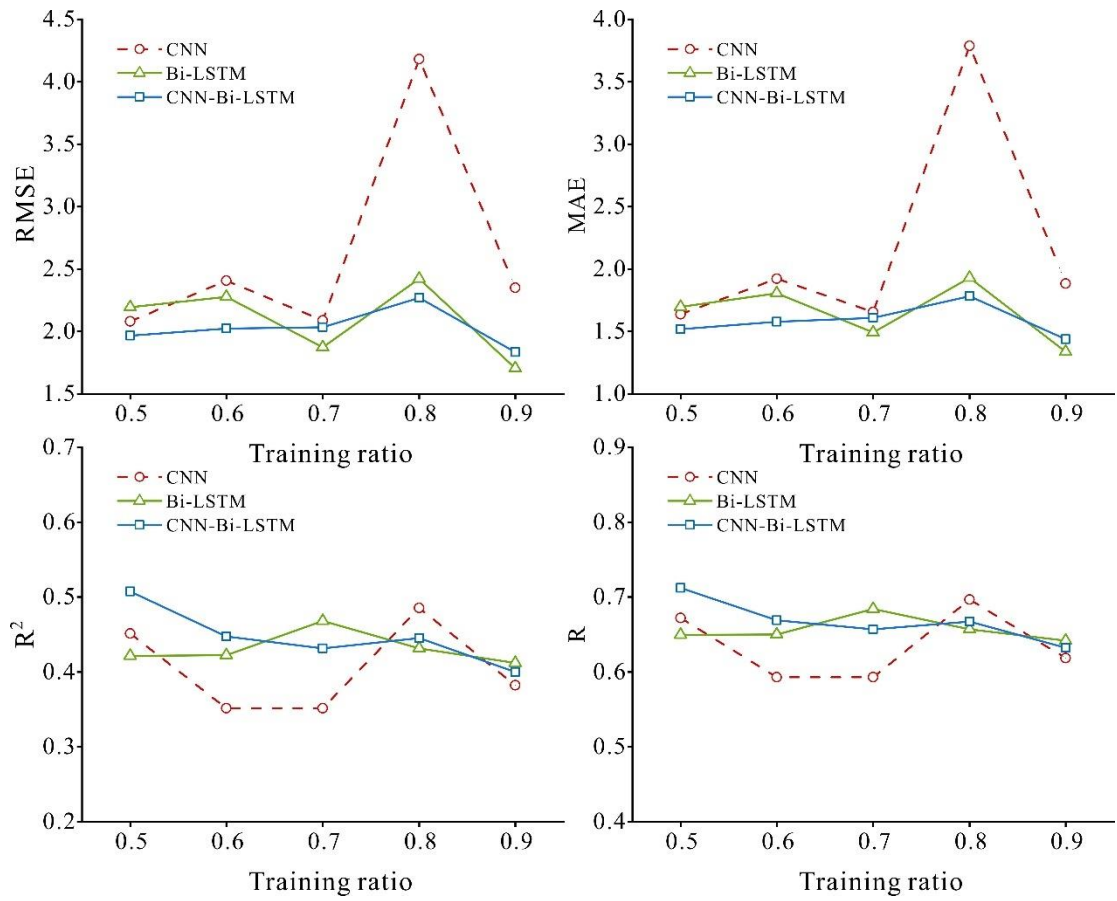
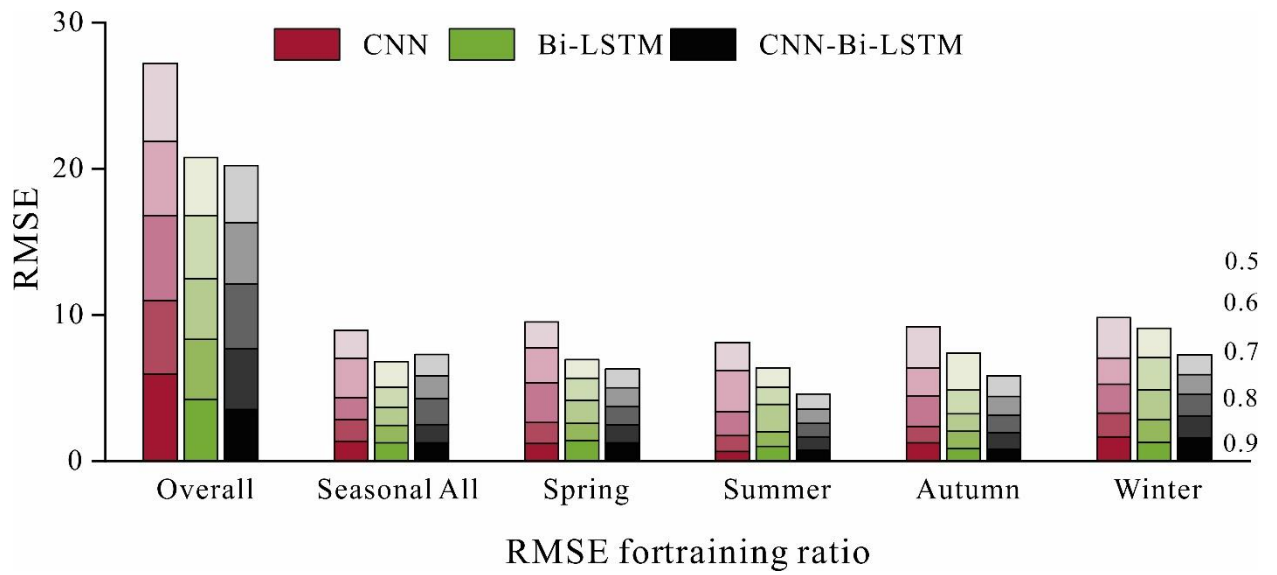


Fig. 6 Overall precipitation $\delta^{18}\text{O}$ forecasting.



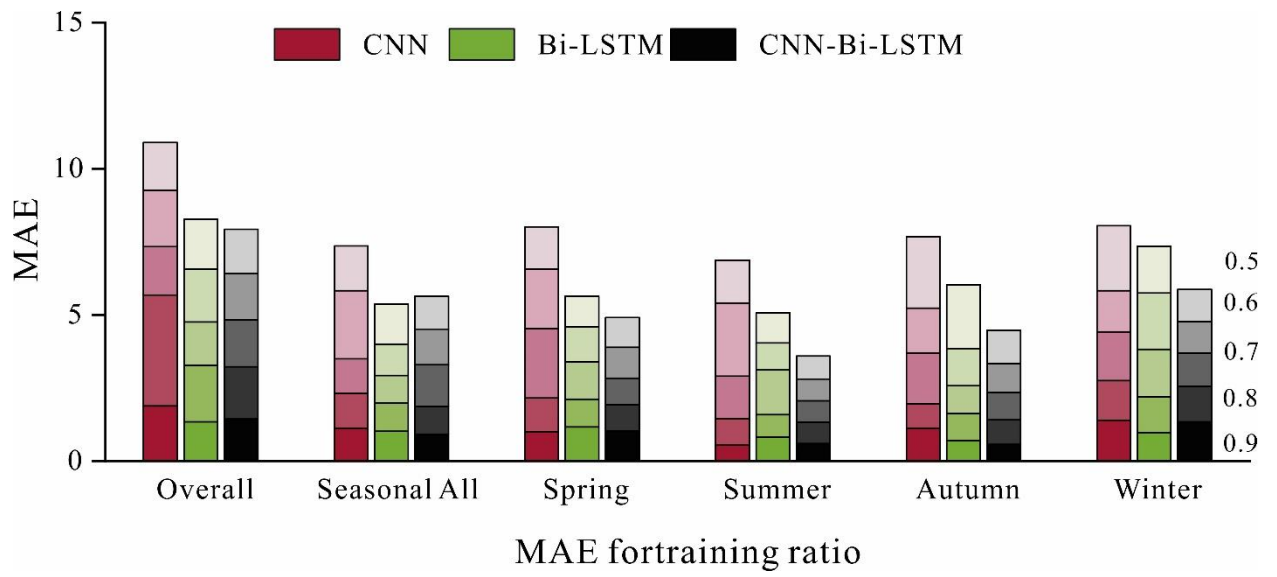


Fig. 7 Seasonal $\delta^{18}\text{O}$ forecasting.

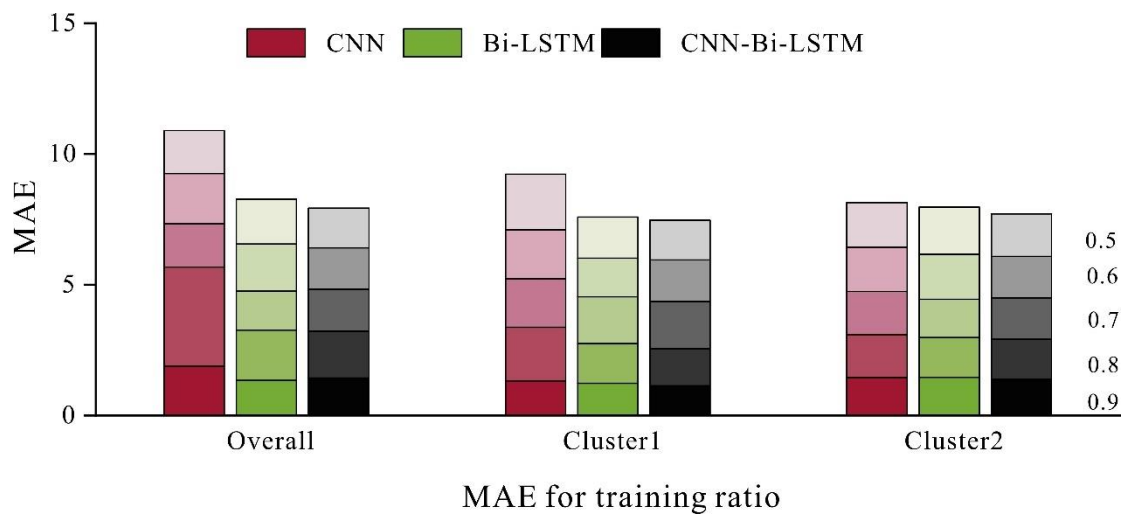
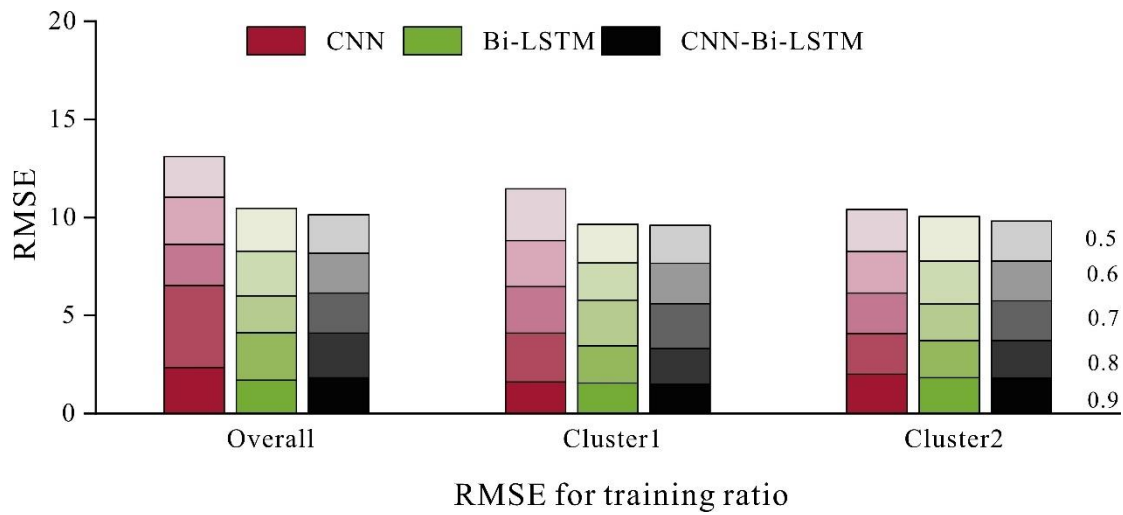


Fig. 8 K-means ++ clustering-based $\delta^{18}\text{O}$ forecasting.

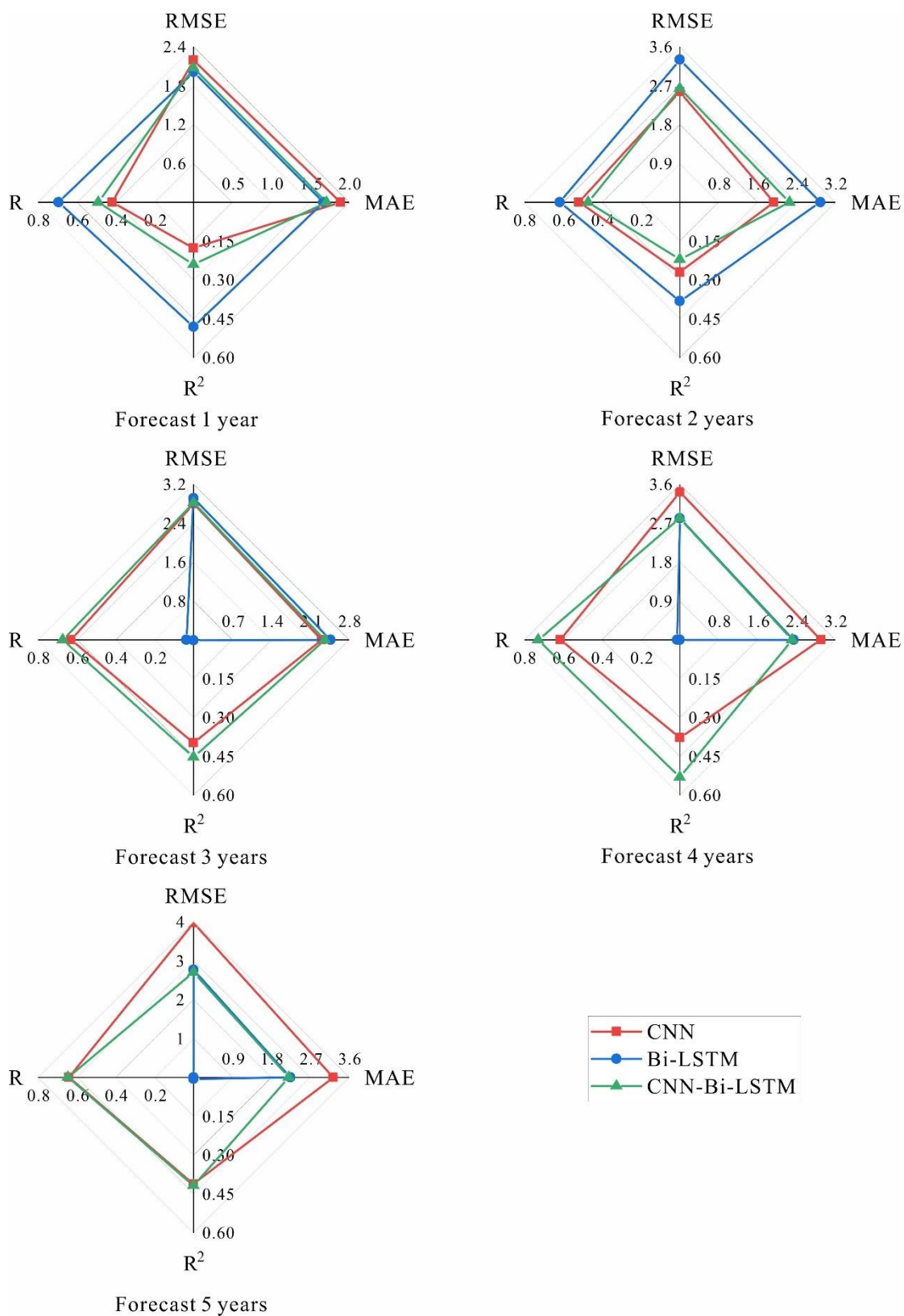
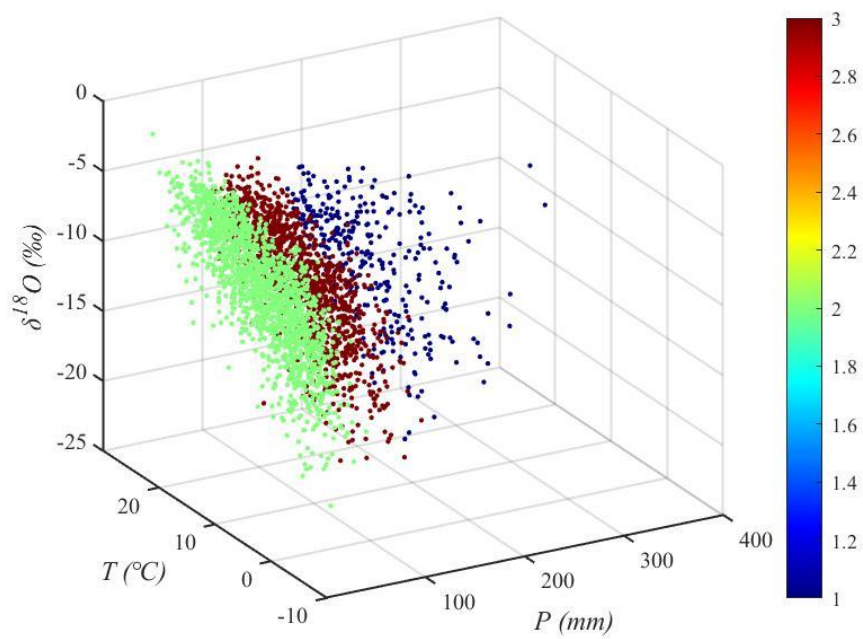
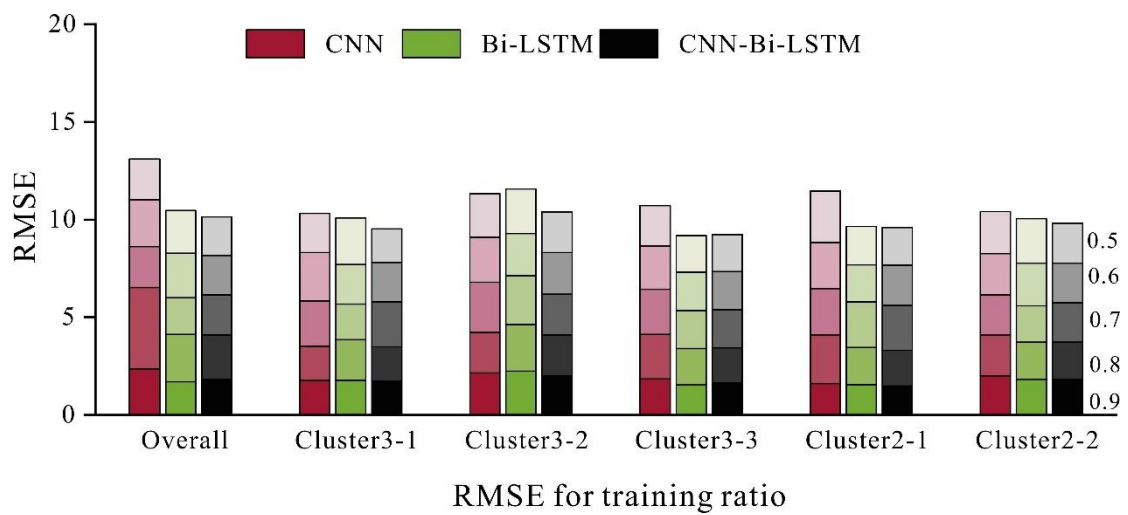
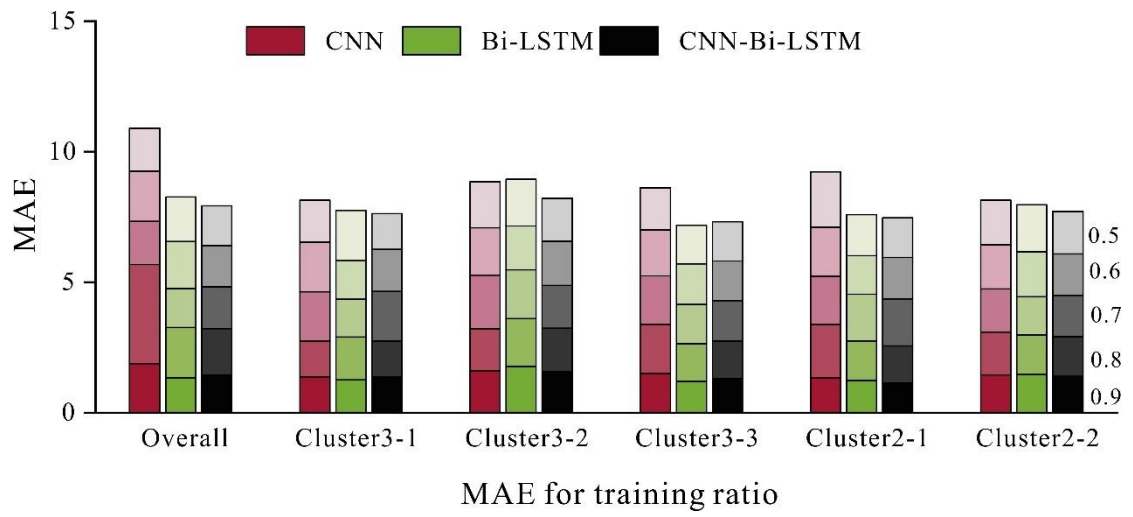


Fig. 9 Comparison of precipitation $\delta^{18}\text{O}$ forecasting models for station STUTTGART.



(a) Spatiotemporal distribution characteristics of the precipitation $\delta^{18}\text{O}$.





(b) K-means ++ clustering-based $\delta^{18}\text{O}$ forecasting.

Fig. 10 Joint forecasting results of K-means ++ clustering and CNN, Bi-LSTM and CNN- Bi-LSTM models.